

1 Powerful eQTL mapping through low coverage RNA sequencing

2
3 Tommer Schwarz ^{1,2}, Toni Boltz ³, Kangcheng Hou ¹, Merel Bot ⁴, Chenda Duan ⁵, Loes Olde
4 Loohuis ^{7,8}, Marco P. Boks ⁹, René S. Kahn ^{9,10}, Roel A. Ophoff ^{1,3,11}, Bogdan Pasaniuc ^{1,2,3,6}

5
6 1. Bioinformatics Interdepartmental Program, University of California Los Angeles, Los Angeles,
7 CA, USA

8 2. Department of Computational Medicine, David Geffen School of Medicine, University of
9 California Los Angeles, Los Angeles, CA, USA

10 3. Department of Human Genetics, David Geffen School of Medicine, University of California Los
11 Angeles, Los Angeles, CA, USA

12 4. Center for Neurobehavioral Genetics, Semel Institute for Neuroscience and Human Behavior,
13 University of California, Los Angeles, California, USA

14 5. Department of Computer Science, University of California, Los Angeles, Los Angeles, CA USA

15 6. Department of Pathology and Laboratory Medicine, David Geffen School of Medicine,
16 University of California Los Angeles, Los Angeles, CA, USA

17 7. Department of Psychiatry, David Geffen School of Medicine, University of California, Los
18 Angeles, Los Angeles, CA, USA

19 8. Program in Neurobehavioral Genetics, Semel Institute, David Geffen School of Medicine,
20 University of California, Los Angeles, Los Angeles, CA, USA

21 9. Department of Psychiatry, Brain Center University Medical Center Utrecht, University Utrecht,
22 Utrecht, The Netherlands

23 10. Department of Psychiatry, Icahn School of Medicine, Mount Sinai, NY, the United States of
24 America

25 11. Department of Psychiatry, Erasmus University Medical Center, Rotterdam, The Netherlands

26
27 Corresponding authors: Tommer Schwarz (tomschwarz@g.ucla.edu), Bogdan Pasaniuc
28 (pasaniuc@ucla.edu)

29
30
31
32
33
34
35
36
37
38
39
40
41
42
43
44
45
46
47
48

49 **ABSTRACT**

50 Mapping genetic variants that regulate gene expression (eQTL mapping) in large-scale RNA
51 sequencing (RNA-seq) studies is often employed to understand functional consequences of
52 regulatory variants. However, the high cost of RNA-Seq limits sample size, sequencing depth,
53 and therefore, discovery power. In this work, we demonstrate that, given a fixed budget, eQTL
54 discovery power can be increased by lowering the sequencing depth per sample and increasing
55 the number of individuals sequenced in the assay. We perform RNA-Seq of whole blood tissue
56 across 1490 individuals at low-coverage (5.9 million reads/sample) and show that the effective
57 power is higher than that of an RNA-Seq study of 570 individuals at high-coverage (13.9 million
58 reads/sample). Next, we leverage synthetic datasets derived from real RNA-Seq data to explore
59 the interplay of coverage and number individuals in eQTL studies, and show that a 10-fold
60 reduction in coverage leads to only a 2.5-fold reduction in statistical power. Our study suggests
61 that lowering coverage while increasing the number of individuals is an effective approach to
62 increase discovery power in RNA-Seq studies.

63 **KEYWORDS**

64 RNA-Seq, Gene expression, Association testing

65

66 **BACKGROUND**

67 The vast majority of risk loci identified in genome-wide association studies (GWAS) are difficult to
68 interpret as they lie in noncoding regions of the genome. Variants that regulate gene expression
69 abundance, as measured through expression quantitative trait locus (eQTL) studies, provide
70 insightful information about the functional interpretation of GWAS signals ¹⁻². By integrating eQTL
71 associations with GWAS, we can hope to identify target genes that are driving the GWAS signal
72 at a locus ³⁻⁶. RNA sequencing (RNA-Seq) is the state-of-the-art assay for measuring gene

73 expression in bulk tissue and is therefore the assay of choice for eQTL mapping ⁷⁻⁸. However, the
74 high cost of RNA-Seq often limits the sample size and therefore reduces the discovery power of
75 eQTL studies based on RNA-Seq ^{2,6,9}.

76 Traditional RNA-Seq study design prioritizes sequencing depth per individual (targeted levels of
77 coverage in the range of 30-50 million reads) over the number of individuals (samples) included
78 in the study ¹⁰⁻¹². However, given that high levels of coverage per individual limits the sample size
79 of a study, this results in a loss of statistical power in eQTL mapping. Previous studies have
80 established that the low-coverage whole genome sequencing of a larger number of individuals
81 attains increased power of association compared to higher-coverage studies of smaller sample
82 sizes in GWAS ¹³⁻¹⁷. This raises the hypothesis that, similarly as for whole genome sequencing
83 and GWAS, lower coverage RNA-seq with a considerable increase in the number of individuals
84 sequenced could increase power of discovery in eQTL studies ¹⁸⁻²¹. Currently, there is no
85 systematic approach for determining the optimal sample size (in terms of number of sequenced
86 individuals) and coverage to maximize eQTL discovery power.

87 In this work, we perform RNA-Seq in 1490 individuals at a lower coverage (average mapped read
88 depth of 5.9 million reads/sample) and find that eQTL discovery power is better than that of an
89 experiment with a similar budget, but with fewer individuals and higher coverage. Compared to
90 high-coverage RNA-Seq, we find a high degree of consistency in both the gene expression as
91 well as eQTL effects. We assess the interplay of coverage per sample and accuracy of expression
92 estimates using synthetic RNA-Seq datasets generated by the down-sampling of real high-
93 coverage data. Our analyses show that a sequencing experiment conducted with a target
94 coverage of 10 million reads/sample has an average correlation per-gene of 0.40, when compared
95 to an experiment conducted with a target coverage of 50 million reads/sample. We provide
96 evidence to show that under a fixed budget, sequencing at lower coverage levels (< 10 million

97 reads/sample) and increased sample size can boost the effective sample size per unit of cost
98 compared to standard approaches of eQTL study design.

99 **RESULTS**

100 ***Low-coverage RNA-sequencing is accurate for eQTL mapping***

101 To validate the utility of low-coverage RNA-sequencing, we sequenced whole blood tissue from
102 N = 1490 unrelated individuals (**Methods**) (**Supplementary Figure 1A** and **Supplementary**
103 **Figure 1B**). We target a sequencing coverage of 9.5 million reads per sample, yielding M = 5.9
104 million reads mapped to RefSeq genes on average (sd across samples of 1.96 million,
105 **Supplementary Figure 2**). We refer to this dataset as the lower-coverage RNA-Seq, or the M=5.9
106 million reads/sample dataset. We contrast this dataset with an RNA-Seq dataset obtained with a
107 similar budget, but with 2.4-fold higher coverage (M = 13.9 reads) across N = 570 individuals
108 (**Supplementary Figure 1C** and **Supplementary Figure 1D**) ²². We refer to this as the higher-
109 coverage whole blood RNA-Seq, or the M = 13.9 million reads/sample dataset (Table 1).

110 First, we assess the number of genes quantified in the two datasets. We observe 40459 genes
111 with at least one mapped read on average across samples in the whole blood high-coverage
112 dataset, and 27308 genes with at least one mapped read on average across samples in the whole
113 blood low-coverage dataset. Notably, when restricting to protein coding genes with at least one
114 mapped read in both the high-coverage and low-coverage datasets, we find more similar numbers
115 between the data sets, with 18329 and 15605 genes quantified, respectively. This is likely due to
116 the very sparse abundance of the non-protein coding genes, making them less likely to be
117 detected in a lower coverage dataset. Indeed, we observe similar effects across the high vs low
118 coverage datasets when assessing the genes with sufficient expression to be included in eQTL
119 analysis (TPM > 0.1 in 20% of individuals, see **Methods**): 26566 genes (15496 protein coding
120 genes) in high coverage data versus 19039 (13339 protein coding genes) in low coverage data.

121 Most importantly we observe a high correlation in the abundance levels across the two data sets
122 thus demonstrating that high and low coverage recover similar expression ($R^2= 0.91$, **Figure 1A**).
123 Next, we investigate the power of low-coverage RNA-Seq for eQTL mapping. We conducted cis-
124 eQTL mapping with a 1 Mb window using FastQTL, restricting to the 1490 unrelated individuals
125 in the low-coverage RNA-Seq data (**Methods**), to identify 7587 genes (eGenes) with a significant
126 association at FDR correction level of 5%. As expected, eQTL distribution is concentrated at
127 transcription start sites (TSS), with 73% of eGenes TSS within 250kb of the associated SNP
128 (eSNP). Repeating this approach using the high-coverage whole blood data in 570 individuals,
129 we only find 5971 genes with a significant association at FDR correction level of 5%. 4969 of the
130 7587 eGenes found using the low-coverage data are also significant in the high-coverage data.
131 Of these, 2151 of the eGenes are protein coding eGenes that share the same associated eSNP,
132 and we see an extremely high level of concordance between effect sizes for these eGenes across
133 the two datasets ($R^2 = 0.93$, **Figure 1B**). This further indicates that low-coverage RNA-Seq is
134 robust in capturing eQTL effect sizes. 1002 genes were found to be eGenes in the high-coverage
135 eQTL analysis but not in the low-coverage analysis, with 573 (of the 1002) not passing expression
136 levels (TPM >0.1 in 20% individuals) to be included in the low-coverage eQTL analysis; only 234
137 of the 573 were protein coding genes. Similar concordance is observed at the level of p-values
138 for the associations in both datasets (**Figure 1C**). Comparing the p-values for eGenes detected
139 in both eQTL analyses, the corresponding regression line has a slope of 0.39, consistent with
140 lower-coverage dataset having superior statistical power to detect associations over lower-
141 coverage dataset, and consistent with overall number of significant eQTL discoveries. We report
142 the results from using typed SNPs in these eQTL analyses (**Methods**), but observe similar
143 patterns when using the full set of imputed SNPs.
144 To further validate the performance of eQTL analysis using lower coverage RNA-Seq (coverage
145 5.9M, n = 1490), we compared the resulting eQTLs to the ones found by GTEx consortium in

146 whole blood ¹² (**Supplementary Figure 3**). Restricting to the 12247 protein coding genes with
147 sufficient expression to be included in both studies (> 0.1 TPM in 20% of samples) we find that
148 4529 out of the 5957 protein coding genes (76%) with a significant association using the lower-
149 coverage data also had a significant association in GTEx, correcting at an FDR level of 5%.
150 Further restricting to eGenes with the same leading SNP in both of these datasets (140 genes)
151 (**Figure 1D**), we observe a correlation (R^2) of 0.85 between their effect sizes. Looking into the
152 1428 protein coding genes with a significant association in eQTL analysis using the lower-
153 coverage RNA-Seq but not in GTEx using an FDR cutoff of 5%, we observe that 372 have
154 significant association in GTEx using an FDR cutoff of 10%. To further ensure that these eGenes
155 are not false positives, we compare the set of 1428 genes with eQTL analysis conducted by the
156 eQTLGen Consortium ²³ and find that all but 190 of these genes have been found to have a
157 significant association in eQTLGen. This suggests that the additional associations found using
158 lower-coverage data that are not found in GTEx are not false positives, but fall just below the
159 significance threshold in the GTEx analysis.

160 Finally, we explore the impact of RNA-Seq at lower coverages for cell type expression
161 estimation. We use Cibersort ²⁴ to compare cell-type proportion estimates between the lower-
162 coverage data and higher-coverage data (**Methods**). We find that the median estimated cell
163 type proportions are conserved across both datasets, suggesting that deconvolution of cell type
164 specific signal from gene expression profiles of whole blood samples is not impacted when
165 coverage is reduced by half (**Supplementary Figure 7**).

166 ***Impact of RNA-seq coverage on eQTL power***

167 Having demonstrated the accuracy of low-coverage RNA-Seq in eQTL mapping in real data, we
168 next focused on exploring the interplay of number of individuals and coverage for optimizing
169 power for discovery. As simulating RNA-Seq data is challenging ²⁵⁻²⁶, we down-sample reads from
170 higher-coverage RNA-Seq data to create synthetic datasets at various coverages (**Methods**). We

171 observe that with just a fraction of the reads, it is still possible to estimate gene expression (**Figure**
172 **2A**). For example, using just 10% of the data (5.0 million reads/sample) retains a per gene R^2 of
173 0.40, on average. The results from our analyses using these synthetic lower-coverage RNA-Seq
174 datasets suggest that under simplified settings of no per-sample library preparation cost, the
175 statistical power in an association study can be increased up to fourfold by spending more
176 resources on increasing sample size and fewer resources on increasing coverage. In practice,
177 increasing the number of samples in an RNA-Seq study leads to increased library preparation
178 costs, making the increase in obtainable statistical association power less obvious.

179 It has been established that statistical power in association studies is a function of sample size,
180 phenotype measurement accuracy, and genotype measurement accuracy^{13,19,29}. This means that
181 the power of a study with sample size N and estimated gene expression is approximately the
182 same as the power of a study with sample size N, using the true gene expression measurements
183 (**Methods**). In this scenario, R^2 is the correlation between the true expression and the expression
184 estimates. We therefore report the squared correlation (R^2) between synthetic datasets at various
185 coverages and the full data at an average of 50 million reads/sample (which is assumed to be the
186 true gene expression). While these results show the mean R^2 for all genes obtained under one
187 synthetic dataset (one draw) per coverage level, we find that the synthetic datasets are consistent
188 across multiple draws at the same coverage level (**Supplementary Figure 4A**) and each show
189 similar correlations with the ground truth gene expression (**Supplementary Figure 4B**).

190 Next, we quantified how well lower-coverage RNA-Seq can be used to detect eGenes³⁰. We
191 explore the number of genes with significant associations after FDR correction at 5% under
192 various levels of simulated coverage (**Figure 2B**). Using synthetic data, as the number of reads
193 per sample decreases, we find that many eGenes are still detectable. For example, at 10 million
194 reads per sample, just 20% of the full coverage, 60% of the eGenes are still detected. In the
195 context of eQTL studies, synthetic RNA-Seq supports the idea that sequencing at lower

196 coverages over a higher number of individuals is a promising approach to boosting statistical
197 power.

198 Finally, we explore the estimation accuracy in the synthetic data as a function of relative gene
199 expression abundance, since less abundant genes may not be captured altogether at lower
200 sequencing coverages. We stratify genes into five groups based on their relative expression in
201 the full dataset ($M=50.3$ million reads/sample) and report the R^2 for genes in each of these groups
202 in synthetic data (**Figure 2C**). We observe that in the synthetic RNA-Seq dataset at 10 million
203 reads/sample, we capture expression of highly expressed genes better than lower expressed
204 genes. Specifically, for genes in the lowest through the highest quintiles of relative gene
205 abundance, we find the average correlation (R^2) to the ground truth of expression to be 0.36, 0.44,
206 0.61, 0.73, 0.86, respectively. We observe the same effect for synthetic datasets at coverages of
207 1 million reads/sample and 25 million reads/sample (**Supplementary Figure 5A** and
208 **Supplementary Figure 5B**). These results suggest that the ability to achieve similar power in
209 eQTL analysis studies will differ per gene, and is a function of relative expression. We further
210 investigate the properties of genes with quantification accuracy influenced by coverage levels of
211 sequencing and find that that protein coding genes are more accurately quantified at lower
212 coverage levels (**Supplementary Figure 6A**). Conversely, the number of transcripts per gene,
213 gene length, and GC content do not appear to be factors that broadly influence the gene
214 quantification accuracy when sequencing coverage is reduced (**Supplementary Figure 6B**,
215 **Supplementary Figure 6C**, and **Supplementary Figure 6D**).

216 ***Optimal association power for eQTLs is attained at lower coverage with a larger number
217 of samples***

218 In the context of reducing experimental costs, we explored the trade-off between the number of
219 samples sequenced and the average coverage per sample. We evaluated the expected effective
220 sample size obtained with lower coverage per sample and compared this with a conventional

221 approach of 50 million reads/sample. We down-sample reads (as described in Section 1 and
222 **Methods**) from a high-coverage RNA-Seq experiment derived from Fibroblast tissue in order to
223 create lower-coverage RNA-Seq synthetic data. This is done to match actual low coverage
224 sequencing as closely as possible. To evaluate the relationship between cost, coverage, and
225 sample size, we use the following equation to model the budget: $B = n * a + \frac{n * b * c}{d}$

226 Where B is the cost/budget (in US dollars), a is the library preparation cost per sample, b is the
227 target coverage of each sample (in millions of reads), c is the cost per lane (which contains d
228 million reads), and d is the number of reads per sequencing lane (in millions). We compute the
229 effective sample size of an eQTL study as a function of average coverage, which determines the
230 number of samples sequenced under a fixed budget (**Figure 3A**). As an example, at a fixed
231 budget of \$300,000, the highest effective sample size is achieved by sequencing 2045 individuals
232 using 10 million reads per sample, which leads to a corresponding effective sample size of 1107.
233 An experiment achieving the sample effective sample size, using 50 million reads per sample,
234 would cost \$426,564 ($N = 1107$, $R^2 = 1.0$). Therefore, by lowering the coverage of each sample
235 and increasing sample size, we achieve the same effective sample size at just 70.3% of the cost.

236 In practice, it is common to observe a considerable discrepancy between the target number of
237 reads in an experiment and the number of reads that successfully map to genes. This can be
238 attributed to different library prep techniques, quality of samples, or tissue type. To show how
239 mapping rate can influence the effective sample size of an experiment, we model effective sample
240 size with varying levels of mapping rates (**Methods**). As expected, we observe that as the
241 mapping rate increases, there is a corresponding increase in effective sample size (**Figure 3C**).
242 We provide a webtool as a practical approach for selecting cost-effective designs for maximizing
243 eQTL power: <https://tomschwarz.shinyapps.io/RNASeqCoverageCalculator/>.

244 With a budget of ~\$300k and an expected mapping rate of 0.60 (chosen based on mapping rate
245 of similar experiments using TruSeq Stranded plus rRNA and GlobinZero in whole blood tissue),
246 we see the maximum effective sample size would be achieved at a target coverage of 7 million
247 reads per sample, including 2227 individuals in the study. We estimate that achieving the same
248 effective sample size using data with 50 million reads per sample would cost ~\$500k (N = 1328),
249 or 1.78x the cost of sequencing 2227 individuals at a coverage of 7 million reads/sample. To
250 explore other cost scenarios we provide a webtool we created a webtool where one can enter
251 budget, costs, and other details about the experiment, in order to see how to achieve optimal
252 effective sample size (<https://tomschwarz.shinyapps.io/RNASeqCoverageCalculator/>).

253 **DISCUSSION**

254 In this work, we generate RNA-Seq data at a lower coverage than typically used in eQTL studies
255 (5.9M reads/sample) and demonstrate how this approach boosts effective sample size per unit
256 cost in an association study. To further validate this approach, we use synthetic RNA-Seq data to
257 show that the optimal level of coverage in an RNA-Seq project for the purpose of identifying eQTL
258 associations is lower than is commonly practiced ¹⁰⁻¹². Based on our findings, we recommend
259 increasing sample size while lowering sequencing depth per sample in order to achieve optimal
260 statistical power in association studies.

261 We conclude with some notes, caveats, and future directions. First, synthetic RNA-Seq via
262 downsampling reads is potentially limited in several ways. These synthetic datasets of lower
263 coverage RNA-Seq are created by uniformly sampling from real RNA-Seq data with an average
264 of 50 million reads mapped per sample. However, in practice, it is possible that sequencing biases
265 are not captured by uniform sampling due to the different experimental setup compared to the
266 dataset from which we sample ²⁷. Additionally, these synthetic datasets are based on data
267 obtained from fibroblast tissue with different transcriptomic profiles from whole blood, potentially
268 influencing the sequencing depth required to detect associations with gene expression. Finally,

269 this approach is optimized for eQTL discovery. Other mechanisms that are detected using RNA-
270 Seq, such as RNA splicing, have different mechanisms and will likely have different optimal
271 coverages for detection. The fact that we identify different sets of eGenes depending on which
272 gene expression measurements we consider (GTEX vs eQTLGen vs lower-coverage RNA-Seq),
273 shows that we need to increase cohort sizes in order to fully understand the connection between
274 genetics and gene expression in blood. Furthermore, the results in **Figure 3A** (figure showing
275 effective sample size at various coverages) indicate that even including 1490 individuals under
276 this fixed budget is not enough to achieve the optimal effective sample size. Current approaches
277 are not sufficient to understand the full landscape of eQTLs in whole blood tissue, even while only
278 considering a single genetic ancestry group. We compare the eGenes identified by GTEx,
279 eQTLGen, and the lower-coverage RNA-Seq (**Supplementary Figure 8**) and find that no single
280 study is sufficient in capturing all of the associations in whole blood. As observed in GWAS, much
281 larger sample sizes including far more ancestral diversity in these samples will enable discovery
282 of novel associations in transcriptomics. Including non-European populations and considering the
283 temporal aspect of gene expression will help us gain a more complete understanding of the blood
284 transcriptome landscape in the entire population.

285 **CONCLUSIONS**

286 In summary, we show that reducing coverage and increasing the number of samples in an eQTL
287 study is a valid approach for increasing effective sample size of the association study. We use
288 both real and synthetic RNA-Seq data to confirm the benefit of increased sample sizes in eQTL
289 studies. This approach can be applied to any dataset for which genotypes are available and will
290 help scientists optimize resources when measuring gene expression for the purpose of integration
291 with genetics. We provide an online tool to assist with improved design of eQTL studies at
292 <https://tomschwarz.shinyapps.io/RNASeqCoverageCalculator/>.

293

294 **METHODS**

295 **Cohort Description**

296 The samples included are from a study with individuals ascertained for bipolar disorder (BP). The
297 cohort consists of 916 individuals with BP, 358 controls, and 216 relatives of the individuals with
298 BP.

299 **Connection between effect size and R^2**

300 If g is the genotype at the SNP that we are testing for associations, and β is the effect size of that
301 SNP when regressing on the true gene expression, y , and $\hat{\beta}$ is the effect size of that SNP when
302 regressing on the estimated gene expression, \tilde{y} . The relationship between y and \tilde{y} is as follows
303 that $r^2 = \text{corr}(y, \tilde{y})$. It follows that the estimates of effect size for a SNP on the true gene
304 expression, $\hat{\beta}$, are related to the estimate of effect size for a SNP on the estimated gene
305 expression, $\tilde{\beta}$ as $\hat{\beta} = \text{cov}(g, \tilde{y}) = \text{cov}(g, ry + \varepsilon) = \text{cov}(g, ry) + \text{cov}(g, \varepsilon) = r\hat{\beta}$ where ε is a
306 random variable with mean 0 and variance 1. The association test statistics at low-coverage is
307 $x_{ground} = N\text{cor}^2(g, y)$ thus implying that the association statistic at low coverage
308 is $x_{low-coverage} = N\text{cor}^2(g, \tilde{y}) = N\hat{\beta}^2 = N(r\hat{\beta})^2 = r^2 * N\text{cor}^2(g, y) = r^2 x_{ground}$

309 **Budget model**

310 We modeled the cost of a large-scale bulk RNA-Seq experiment based on parameters from two
311 different library prep techniques: (1) TruSeq Stranded plus rRNA and GlobinZero and (2) TruSeq
312 Stranded polyA selected, both from the UCLA Neuroscience Genomics core. Cost, or B , is a
313 function of the following: a , the library preparation cost per sample, b , which is the target coverage
314 of each sample (in millions of reads), c , the cost per lane (which contains d million reads), and d
315 is the number of reads per sequencing lane (in millions). Altogether, we model the budget as $B =$

$$316 n * a + \frac{n * b * c}{d}$$

317 **Genotyping pipeline**

318 Genotypes for the low-coverage whole blood samples were obtained from the following platforms:
319 OmniExpressExome (N = 810), PSYCH (N = 523), and COEX (N = 163). Given that the SNP-
320 genotype data for both the fibroblast and whole blood samples came from numerous studies using
321 various genotyping platforms (including GSA, Illumina550, OmniExpress Exome, COEX, and
322 PsychChip) the number of overlapping SNPs across all platforms was < 80k, prompting us to
323 perform imputation separately for each genotyping platform. Genotypes were first filtered for
324 Hardy-Weinberg equilibrium p value < 1.0e-6 for controls and p value < 1.0e-10 for cases, with
325 minor allele frequency (MAF) > 0.01, leaving 148613 typed SNPs.

326 Genotypes were imputed using the 1000 Genomes Project phase 3 reference panel ³³ by
327 chromosome using RICOPILI v.1 ³⁴ separately per genotyping platform, then subsequently
328 merged. Imputation quality was assessed by filtering variants where genotype probability > 0.8
329 and INFO score > 0.1, resulting in 2289732 autosomal SNPs. We restricted to only autosomal
330 due to sex chromosome dosage, as commonly done ¹².

331 **Synthetic low coverage RNA-Seq**

332 We use high-coverage RNA-Seq (average of 50 million reads/sample, TruSeq Stranded plus
333 rRNA and GlobinZero library prep) from a set of 152 cell lines derived from human fibroblast cells.
334 We assume this to be the ground truth of gene expression. We used seqtk
335 (<https://github.com/lh3/seqtk>) to randomly sample reads at various coverages, uniformly. We
336 performed five iterations of downsampling at each level of coverage in order to account for
337 potential variability in the sampling and sequencing errors.

338 **RNA-Seq processing pipeline**

339 We used FASTQC to visually inspect the read quality from the lower-coverage whole blood RNA-
340 Seq (5.9M reads/sample) and the higher-coverage fibroblast RNA-Seq (13.9M reads/sample).
341 We then used kallisto to pseudoalign reads to the GRCh37 transcriptome and quantify estimates
342 for transcript expression. We aggregated transcript counts using scripts from the GTEx
343 consortium (<https://github.com/broadinstitute/gtex-pipeline>) ¹².

344 **cis-eQTL mapping**

345 Excluding related individuals ($\pi_{\text{hat}} > 0.2$) from the analysis, we perform cis-eQTL analysis
346 mapping using FastQTL³⁰, using a defined window of 1 Mb both up and downstream of every
347 gene's TSS, for sufficiently expressed genes. We run the eQTL analysis in permutation pass
348 mode (1000 permutations, and perform multiple testing corrections using the q-value FDR
349 procedure, correcting at 5% unless otherwise specified. We then restrict our associations to the
350 top (or leading) SNP per eGene.

351 **Cell type proportion estimation**

352 We estimate the proportion of cell types of both the lower-coverage and higher-coverage bulk
353 whole blood RNA-seq datasets using CIBERSORTx³⁵ with batch correction applied and LM22
354 signature matrix as the reference gene expression profile. The LM22 signature matrix uses 547
355 genes to distinguish between 22 human hematopoietic cell phenotypes.

356 **R^2 adjustment**

357 To account for the variability in mapping rate across different library prep techniques³⁷ and
358 different tissue types, we look at the mean R^2 at the expected coverage, which is calculated as
359 *expected coverage = target coverage * estimated mapping rate*. Using mean R^2 values from
360 comparing lower-coverage synthetic RNA-Seq to higher-coverage RNA-Seq real data, we fit a
361 log curve to estimate the adjusted mean R^2 (R^2_{adj}) at the expected coverage.

362 **Effective Sample Size**

363 Under a fixed-budget setting, we calculate effective sample size (N_{eff}) for a given coverage using
364 the adjusted mean R^2 (R^2_{adj}) and the number of samples included at a given coverage level (N)

$$365 N_{\text{eff}} = R^2_{\text{adj}} * N$$

366 **DECLARATIONS**

367 **Ethics approval and consent to participate**

368 The authors assert that all procedures contributing to this work comply with the ethical standards
369 of the relevant national and institutional committees of human experimentation and with the
370 Helsinki Declaration of 1975, as revised in 2008.

371 **Consent for publication**

372 Not applicable.

373

374 **Availability of data and materials**

375 Gene expression data will be made available upon publication

376

377 **Competing interests**

378 All authors declare they have no competing interest

379

380 **Funding**

381 T.S. was supported by the National Institute of Neurological Disorders and Stroke of the National
382 Institutes of Health under Award Number T32NS048004. T.B. was supported by the NIH (grant
383 number 5T32HG002536-19). This research was supported by the National Institute of Mental
384 Health of the National Institutes of Health under Award number 5R01MH115676-04. The content
385 is solely the responsibility of the authors and does not necessarily represent the official views of
386 the National Institutes of Health.

387

388 **Author Contributions**

389 T.S., B.P., and R.O. initialized the study. B.P. and R.O. directed and supervised the project. R.O.,
390 R.K., and M.P.B. collected samples. M.B. prepared samples for sequencing. Bioinformatics
391 analysis was conducted by T.S., T.B., K.H., C.D., and L.O.L. . The first draft of the manuscript
392 was drafted by T.S. and all authors contributed to editing, revisions, and approval.

393

394 **Acknowledgements**

395 We thank the study subjects for their willingness to provide specimens and clinical data. We thank
396 Yi Ding, Kathryn Burch, Ruthie Johnson, Arjun Bhattacharya, and Malika Freund for meaningful
397 discussion in helping make this work possible.

398

399

400 **SUPPLEMENTAL INFORMATION**

401

402 **Supplementary Figure 1: Distribution of ancestry among samples.** **(S1A)** MDS plot of 2000
403 samples in 5.9M read/sample cohort. **(S1B)** Distribution of ancestry among sample in 5.9M
404 read/sample cohort. **(S1C)** MDS plot of 759 samples in 13.9M read/sample cohort: Genotype PC1
405 and PC2 are projected onto PCs from 1000 Genomes Project. **(S1D)** Distribution of ancestry
406 among sample in 13.9M read/sample cohort.

407

408 **Supplementary Figure 2: Number of pseudoaligned reads per sample.** **(S2A)** Number of
409 pseudoaligned reads per sample in low-coverage RNA-Seq. **(S2B)** Number of pseudoaligned
410 reads per sample in high-coverage RNA-Seq.

411

412 **Supplementary Figure 3: Real data p-value comparison scatterplot with GTEX**

413

414 **Supplementary Figure 4: Variability in correlations in synthetic data.** **(S4A)** Scatterplot of log
415 TPM of different draws in synthetic data. **(S4B)** Distribution of correlations observed between
416 synthetic lower-coverage RNA-Seq and ground truth.

417

418 **Supplementary Figure 5: Using synthetic data, how well do we capture expression as a function**
419 **of average expression in a given gene.** **(S5A)** Correlation as a function of relative expression, at
420 25 million reads/sample. **(S5B)** Correlation as a function of relative expression, at 1 million
421 reads/sample.

422

423 **Supplementary Figure 6: Using synthetic data, how well do we capture expression in different**
424 **gene categories.** **(S6A)** Using synthetic data, how well do we capture expression as a function of
425 whether a gene is protein coding or not. **(S6B)** Using synthetic data, how well do we capture
426 expression as a function of number of isoforms in a given gene. **(S6C)** Using synthetic RNA-Seq,
427 how well do we capture expression as a function of gene length in a given gene Gene expression
428 estimation accuracy simulated at 10 million reads/sample as a function of relative gene length.
429 **(S6D)** Using synthetic RNA-Seq, how well do we capture expression as a function of GC content.

430

431 **Supplementary Figure 7: Estimation of cell-type proportions.**

432

433 **Supplementary Figure 8: Overlap of significant eGenes using RNA-Seq from three different**
434 **datasets**

435

436

437

438 **REFERENCES**

439 1. Montgomery, S. B. *et al.* Transcriptome genetics using second generation sequencing in
440 a Caucasian population. *Nature* vol. 464 773–777 (2010).

441 2. Pickrell, J. K. *et al.* Understanding mechanisms underlying human gene expression
442 variation with RNA sequencing. *Nature* **464**, 768–772 (2010).

443 3. Mancuso, N. *et al.* Integrating Gene Expression with Summary Association Statistics to
444 Identify Genes Associated with 30 Complex Traits. *Am. J. Hum. Genet.* **100**, 473–487 (2017).

445 4. Gusev, A. *et al.* Integrative approaches for large-scale transcriptome-wide association
446 studies. *Nat. Genet.* **48**, 245–252 (2016).

447 5. Gamazon, E. R. *et al.* A gene-based association method for mapping traits using
448 reference transcriptome data. *Nat. Genet.* **47**, 1091–1098 (2015).

449 6. Zhernakova, D. V. *et al.* Identification of context-dependent expression quantitative trait
450 loci in whole blood. *Nat. Genet.* **49**, 139–145 (2017).

451 7. Wang, Z., Gerstein, M. & Snyder, M. RNA-Seq: a revolutionary tool for transcriptomics.
452 *Nat. Rev. Genet.* **10**, 57–63 (2009).

453 8. Rockman, M. V. & Kruglyak, L. Genetics of global gene expression. *Nat. Rev. Genet.* **7**,
454 862–872 (2006).

455 9. Gallagher, M. D. & Chen-Plotkin, A. S. The Post-GWAS Era: From Association to
456 Function. *Am. J. Hum. Genet.* **102**, 717–730 (2018).

457 10. Hoffman, G. E. *et al.* CommonMind Consortium provides transcriptomic and epigenomic
458 data for Schizophrenia and Bipolar Disorder. *Sci Data* **6**, 180 (2019).

459 11. Franzén, O. *et al.* Cardiometabolic risk loci share downstream cis- and trans-gene
460 regulation across tissues and diseases. *Science* **353**, 827–830 (2016).

461 12. GTEx Consortium. The GTEx Consortium atlas of genetic regulatory effects across
462 human tissues. *Science* **369**, 1318–1330 (2020).

463 13. Pasaniuc, B. *et al.* Extremely low-coverage sequencing and imputation increases power
464 for genome-wide association studies. *Nat. Genet.* **44**, 631–635 (2012).

465 14. Sims, D., Sudbery, I., Ilott, N. E., Heger, A. & Ponting, C. P. Sequencing depth and
466 coverage: key considerations in genomic analyses. *Nat. Rev. Genet.* **15**, 121–132 (2014).

467 15. CONVERGE consortium. Sparse whole-genome sequencing identifies two loci for major
468 depressive disorder. *Nature* **523**, 588–591 (2015).

469 16. Homburger, J. R. *et al.* Low coverage whole genome sequencing enables accurate
470 assessment of common variants and calculation of genome-wide polygenic scores. *Genome
471 Med.* **11**, 74 (2019).

472 17. Rubinacci, S., Ribeiro, D. M., Hofmeister, R. J. & Delaneau, O. Efficient phasing and
473 imputation of low-coverage sequencing data using large reference panels. *Nat. Genet.* **53**, 412
474 (2021).

475 18. Baccarella, A., Williams, C. R., Parrish, J. Z. & Kim, C. C. Empirical assessment of the
476 impact of sample number and read depth on RNA-Seq analysis workflow performance. *BMC*
477 *Bioinformatics* **19**, 423 (2018).

478 19. Pritchard, J. K. & Przeworski, M. Linkage disequilibrium in humans: models and data.
479 *Am. J. Hum. Genet.* **69**, 1–14 (2001).

480 20. Tarazona, S., García-Alcalde, F., Dopazo, J., Ferrer, A. & Conesa, A. Differential
481 expression in RNA-seq: a matter of depth. *Genome Res.* **21**, 2213–2223 (2011).

482 21. Robinson, D. G. & Storey, J. D. subSeq: determining appropriate sequencing depth
483 through efficient read subsampling. *Bioinformatics* **30**, 3424–3426 (2014).

484 22. Krebs, C. E. *et al.* Whole blood transcriptome analysis in bipolar disorder reveals strong
485 lithium effect. *Psychol. Med.* **50**, 2575–2586 (2020).

486 23. Võsa U, Claringbould A, Westra H-J, Bonder MJ, Deelen P, Zeng B, *et al.* Unraveling the
487 polygenic architecture of complex traits using blood eQTL meta-analysis. *bioRxiv*. 447367
488 (2018)

489 24. Chen, B., Khodadoust, M. S., Liu, C. L., Newman, A. M. & Alizadeh, A. A. Profiling
490 Tumor Infiltrating Immune Cells with CIBERSORT. *Methods Mol. Biol.* **1711**, 243–259 (2018).

491 25. Williams, A. G., Thomas, S., Wyman, S. K. & Holloway, A. K. RNA-seq Data: Challenges
492 in and Recommendations for Experimental Design and Analysis. *Curr. Protoc. Hum. Genet.* **83**,
493 11.13.1–20 (2014).

494 26. Frazee, A. C., Jaffe, A. E., Langmead, B. & Leek, J. T. Polyester: simulating RNA-seq
495 datasets with differential transcript expression. *Bioinformatics* **31**, 2778–2784 (2015).

496 27. Bray, N. L., Pimentel, H., Melsted, P. & Pachter, L. Near-optimal probabilistic RNA-seq
497 quantification. *Nat. Biotechnol.* **34**, 525–527 (2016).

498 28. Liu, Y. *et al.* Evaluating the impact of sequencing depth on transcriptome profiling in
499 human adipose. *PLoS One* **8**, e66883 (2013).

500 29. Mandric, I. *et al.* Optimized design of single-cell RNA sequencing experiments for cell-
501 type-specific eQTL analysis. *Nat. Commun.* **11**, 5504 (2020).

502 30. Ongen, H., Buil, A., Brown, A. A., Dermitzakis, E. T. & Delaneau, O. Fast and efficient
503 QTL mapper for thousands of molecular phenotypes. *Bioinformatics* **32**, 1479–1485 (2016).

504 31. Marioni, J. C., Mason, C. E., Mane, S. M., Stephens, M. & Gilad, Y. RNA-seq: an
505 assessment of technical reproducibility and comparison with gene expression arrays. *Genome*
506 **Res.** **18**, 1509–1517 (2008).

507 32. Purcell, S. et al. PLINK: A Tool Set for Whole-Genome Association and Population-
508 Based Linkage Analyses. *The American Journal of Human Genetics* vol. 81 559–575 (2007).

509 33. Consortium, T. 1000 G. P. & The 1000 Genomes Project Consortium. A global reference for
510 human genetic variation. *Nature* vol. 526 68–74 (2015).

511 34. Lam, M. et al. RICOPILI: Rapid Imputation for COnsortias PIpeliNe. *Bioinformatics* **36**,
512 930-933 (2019).

513 35. Newman, A.M. et al. Determining cell type abundance and expression from bulk tissues
514 with digital cytometry. *Nature Biotechnology* **37**, 773-782 (2019).

515 36. Hoffman, G. E. et al. CommonMind Consortium provides transcriptomic and epigenomic data
516 for Schizophrenia and Bipolar Disorder. *Sci. Data* **6**, 180 (2019).

517 37. Aguet, F. et al. Genetic effects on gene expression across human tissues. *Nature* **550**, 204–
518 213 (2017)

519
520 **DISPLAY ITEMS**
521
522

Referred to as:	Coverage (million reads per sample)	Tissue	Number of samples	Library prep method
Lower- Coverage or M=5.9M reads/sample (Whole Blood)	5.9	Whole blood	1490	TruSeq Stranded plus rRNA and GlobinZero
Higher- Coverage M=13.9M reads/sample (Whole Blood) ¹⁹	13.9	Whole blood	570	Meta-analysis of (1) TruSeq Stranded plus rRNA and GlobinZero and (2) TruSeq Stranded polyA selected
High-	50.3	Fibroblast	155	TruSeq Stranded polyA selected

coverage (Fibroblast)				
GTEX ¹²	82	Whole blood	670	TruSeq Non-stranded polyA selected
eQTLGen ¹³	N/A	Whole blood	31684	Meta-analysis consisting of RNA-Seq and microarray

523

524 **Table 1: RNA-Seq datasets discussed in this paper**

525 The coverage refers to the average number of reads that successfully map to the transcriptome,
526 except for GTEX, which refers to the median number of total reads per sample (average
527 mapped not available). Further description of sample overlaps among cohorts in
528 **Supplementary Note**.

529

530

531

	Cost per lane	Cost per sample
Scenario 1	\$1790	\$87
Scenario 2	\$1790	\$30
Scenario 3	\$1790	\$150
Scenario 4	\$1000	\$150

532

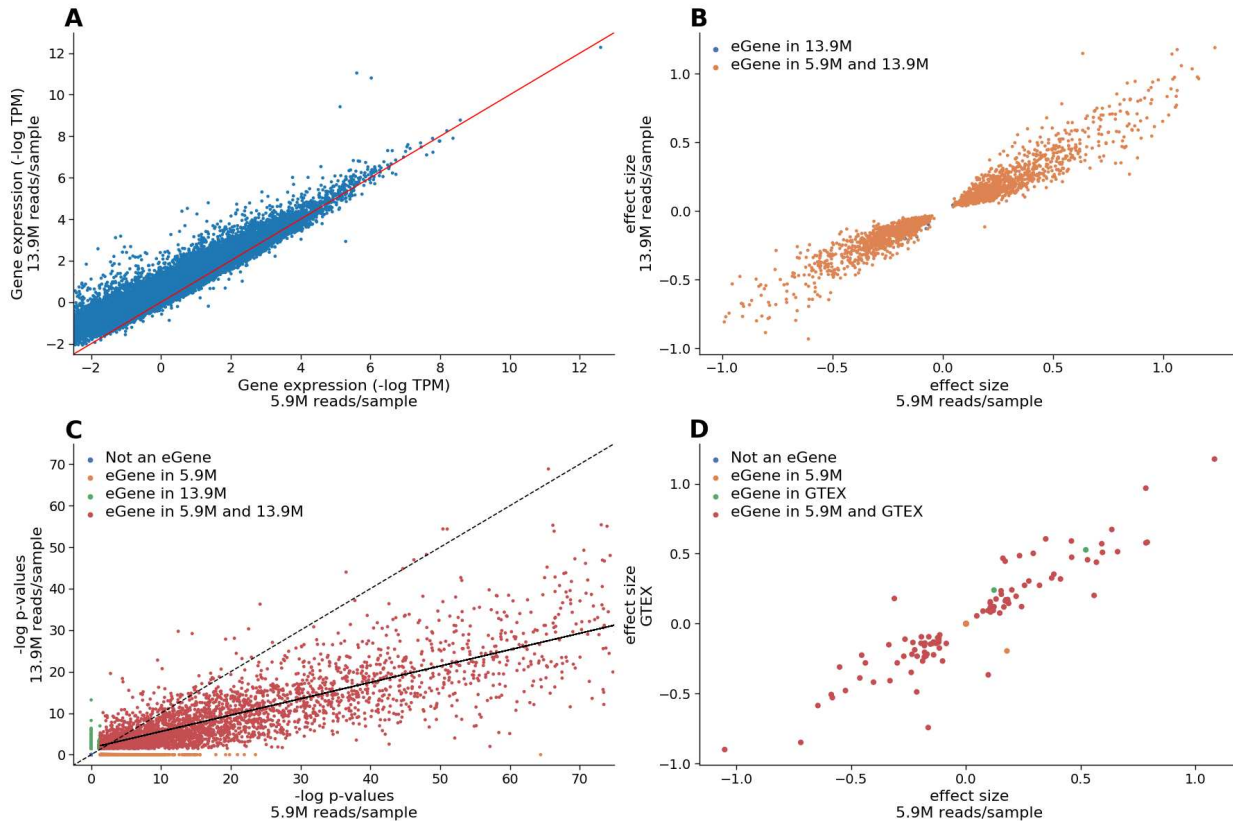
533 **Table 2: Sequencing cost scenarios (Figure 3)**

534 The cost parameters corresponding to the effective sample size scenarios in Figure 3. Cost per
535 sample reflects the cost of library prep to include an additional sample. Cost per lane reflects the
536 cost per sequencing lane, which allows for 300 million reads.

537

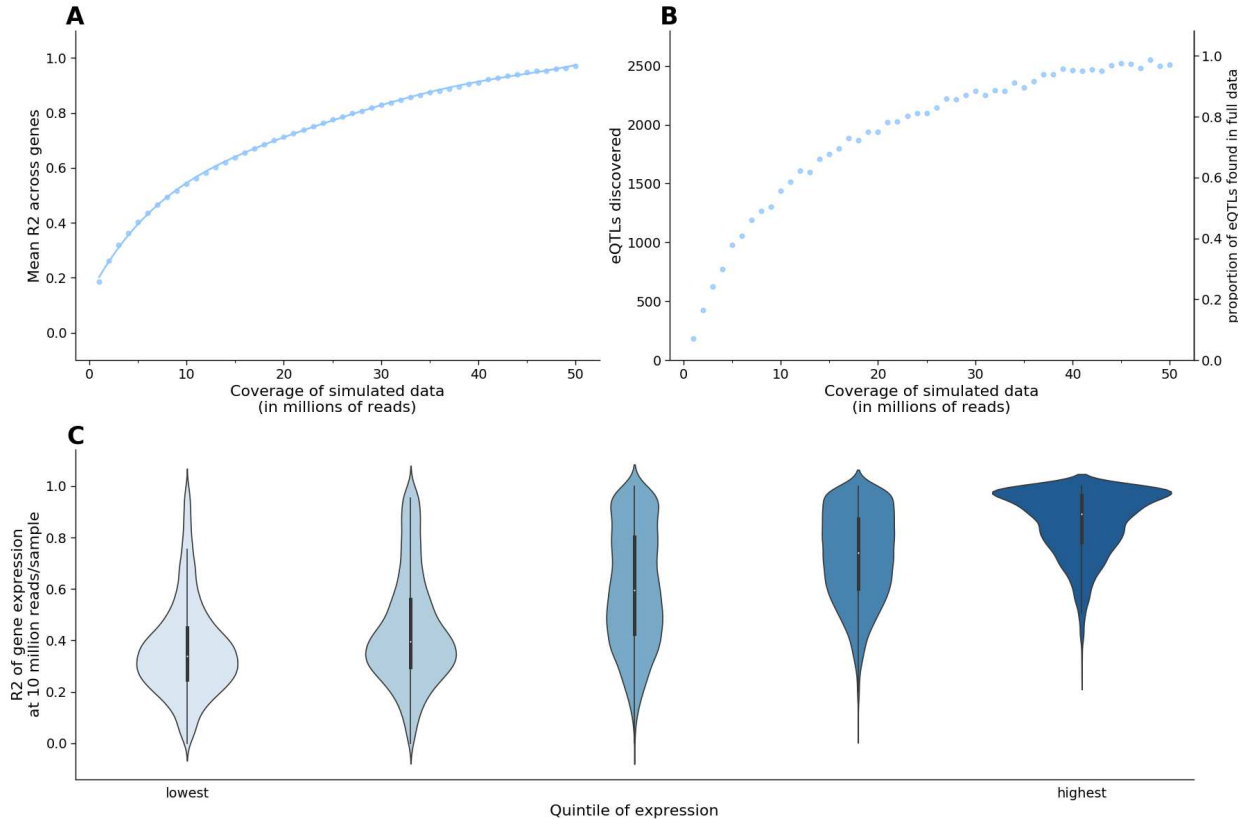
538

539

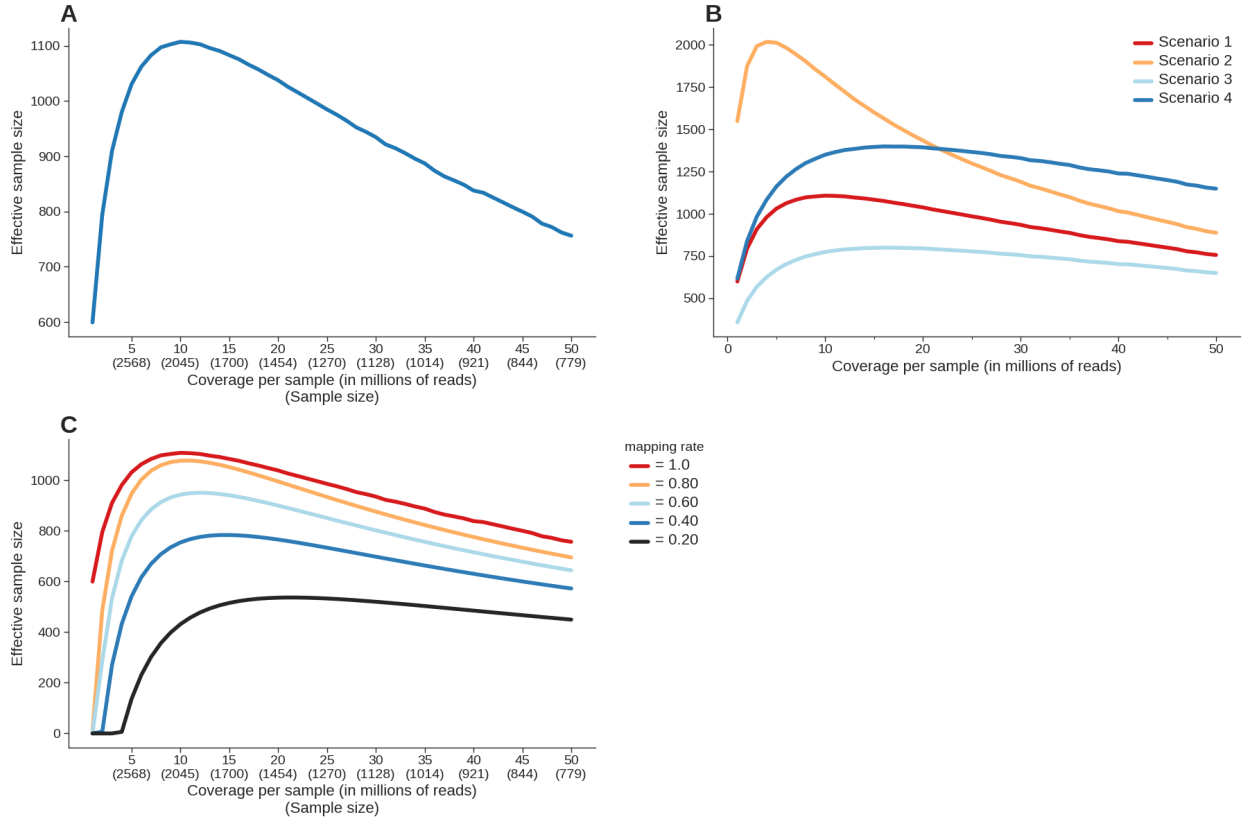


540
541
542
543
544
545
546
547
548
549
550
551
552
553
554
555
556
557
558
559
560
561
562
563

Figure 1: Concordance of eQTL discovery when using lower-coverage RNA-Seq vs higher-coverage RNA-Seq (1A): Restricting to the 20735 genes with sufficient expression levels to be included in eQTL analysis in both the 5.9M read/sample and 13.9M read/sample dataset, comparison of the median expression (log TPM) across samples, of every gene. $R^2 = 0.91$. **(1B):** In real data, scatterplot of effect sizes of most significant eQTL hits for the 2151 protein coding genes with the same eQTL hit in both eQTL analyses performed (low-coverage and high-coverage). On the x-axis, we show the effect sizes for these genes using low-coverage RNA-Seq, on the y-axis we show the effect sizes for these genes using high-coverage RNA-Seq. **(1C):** Real data p-value comparison scatterplot: In real data, scatterplot of -log p-values of most significant eQTL hit for 13950 genes included in both eQTL analyses performed (low-coverage and high-coverage). On the x-axis, we show the -log p-values for these genes using low-coverage RNA-Seq, on the y-axis we show the -log p-values for these genes using high-coverage RNA-Seq. The dotted line shows $y = x$, while the solid line shows the line of best fit for the 3985 protein-coding eGenes with a significant eQTL hit in both datasets. **(1D):** In real data, scatterplot of effect sizes of the most significant eQTL hit for the 140 eGenes with the same leading SNP identified in both eQTL analyses performed (lower-coverage RNA-Seq with 5.9M reads/sample and GTEX). On the x-axis, we show the effect size for these eGenes from eQTL analysis conducted using the 1490 individuals of EUR ancestry and imputed genotypes, and on the y-axis we show the effect sizes for these eGenes from eQTL analysis published by the GTEX Consortium.



564
565
566 **Figure 2: Synthetic lower-coverage RNA-Seq captures expression signal (2A):** On the x-axis, we
567 show the level of simulated coverage, and on the y-axis we show the mean Pearson correlation
568 of every gene. We calculate this value by finding the R^2 values for the TPM values of each of
569 45,910 genes across 155 samples between the high coverage data (average of 50 million reads
570 per sample) and the simulated data, and reporting the mean R^2 value per gene. **(2B):** For a fixed
571 number of individuals, absolute number and percentage of eGenes captured at 5% FDR, for
572 synthetic RNA-Seq at varying levels of coverage. **(2C):** Gene expression accuracy as a function
573 of relative gene expression observed in actual RNA-Seq data with 50 million reads/sample.
574 23,540 genes (with average expression < 0.1 TPM) are divided into five ascending quintiles of
575 expression based on their average expression in 155 samples.
576
577



578
579
580
581
582
583
584
585
586

Figure 3: Effective sample size under various budget parameters. (3A): Effective sample size in RNA-Seq under a fixed budget (\$300,000) as a function of the number of samples and the resulting coverage. Cost assumptions: \$87 per library prep per sample, \$1790 per lane of sequencing (300 million reads). **(3B):** Effective sample size in RNA-Seq under a fixed budget (\$300,000) as a function of the number of samples and the resulting coverage. Cost assumptions vary and are reflected in Table 2. **(3C):** Effective sample size under a fixed budget (\$300,000) as a function of the number of samples and the results coverage. A global mapping rate parameter is used to simulate actual experimental conditions (Methods).